SUPPORTING INFORMATION

Novel fluorescent self-assembling material with gel properties: ion recognition and energy transfer

College of Chemistry and Chemical Engineering, Ningxia Normal University, Guyuan 756000, People's Republic of China.Fax: 86 954 2079637; Tel: 86 954 2079637; E-mail: maxinxian@163.com

Experimental section

Materials

Unless otherwise noted, all reactions were performed in air atmosphere. Deionized water was used for the whole experiment process. The commercially available reagents, metal salts and organic solvents were used as received unless otherwise specified purification.

Characterizations

All yields were given as isolated yields. The ^{1}H and ^{13}C NMR spectra were recorded on a Bruker 400 MHz spectrometer. Mass spectra were carried out by a Bruker solanX 70 FT-MS mass spectrometer equipped with ESI interface and ion trap analyzer. The infrared spectra were recorded on a Thermo Scientific Nicolet iS5 FT-IR spectrophotometer. Ultraviolet-visible (UV-vis) spectra were recorded on a Shimadzu UV-1750 spectrometer. The measurements of steady-state luminescence were recorded with a Shimadzu RF-5301PC spectrometer. The morphologies of the as-synthesized samples were characterized with a SM-74190UEC SEM using an accelerating voltage of 10kV. X-ray diffraction patterns (XRD) were determined with a X' Pert PRO diffractometer using Cu-Kα radiation over the 2θ range of 5-90°. The quantum yields were carried out on a FLS980 instrument with the integrating sphere.

Synthesis
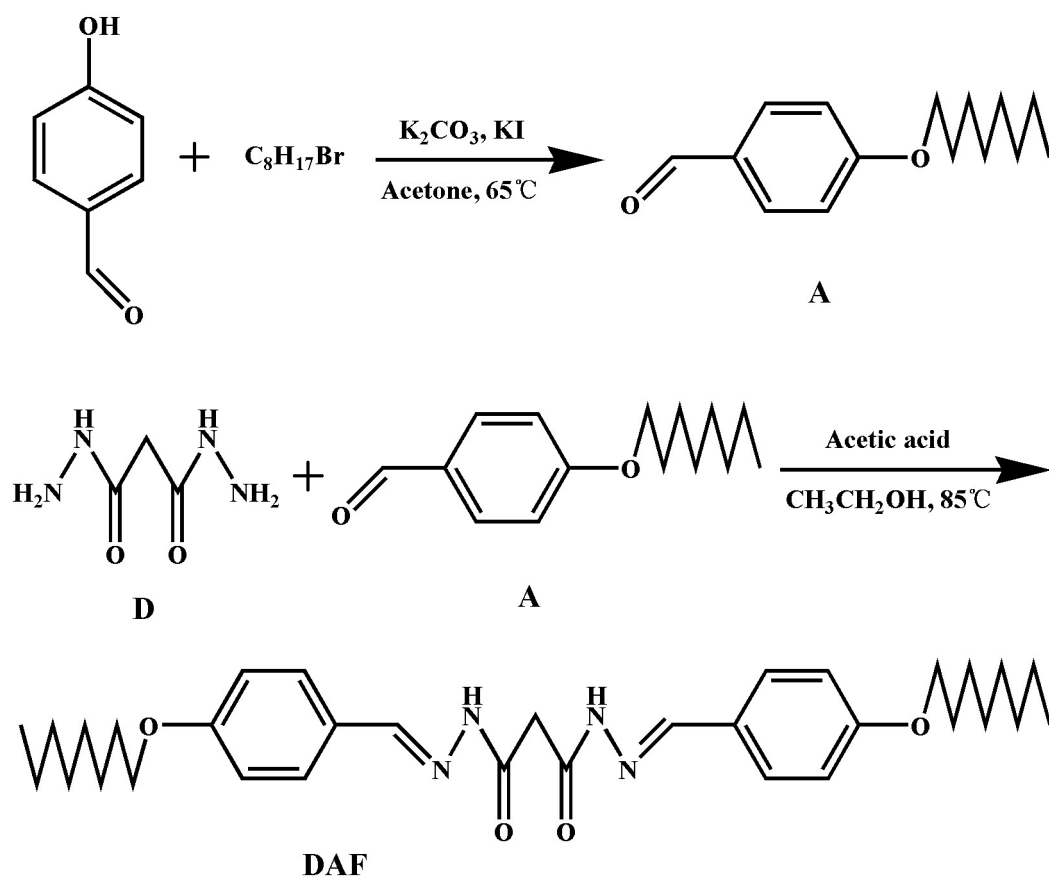
**Scheme S1** The synthetic route of **DAF**

Synthesis of DAF

As shown in Scheme S1, 4-n-Octyloxybenzaldehyde (A) was prepared by etherification reaction. And then, 4-n-Octyloxybenzaldehyde (A) (2.5 mmol) and Malonic dihydrazide (D) (1 mmol) were dissolved in appropriate ethanol (25 mL) and stirred at 85 °C for 10 h. A small amount of acetic acid was added as the catalyst. After cooling to room temperature, the reaction mixture was filtered. Then it was washed three times with hot absolute ethanol and recrystallized with DMF/H_2O to give a faint yellow powder product DAF (0.384 g) in 71% yield. ^{1}H NMR (400 MHz, DMSO-d_6) δ (ppm): 11.46-11.30 (d, 2H, N–H), 8.16-7.89 (d, 2H, N=CH), 7.64-6.81 (m, 8H, ArH), 3.99-3.56 (m, 6H); ^{13}C NMR (150 MHz, DMSO-d_6) δ (ppm): 169.11, 159.97, 142.49, 128.64, 128.37, 126.83, 114.76, 114.62, 67.61, 41.35, 31.29, 28.79, 28.72, 28.64, 25.54, 22.14, 13.99.
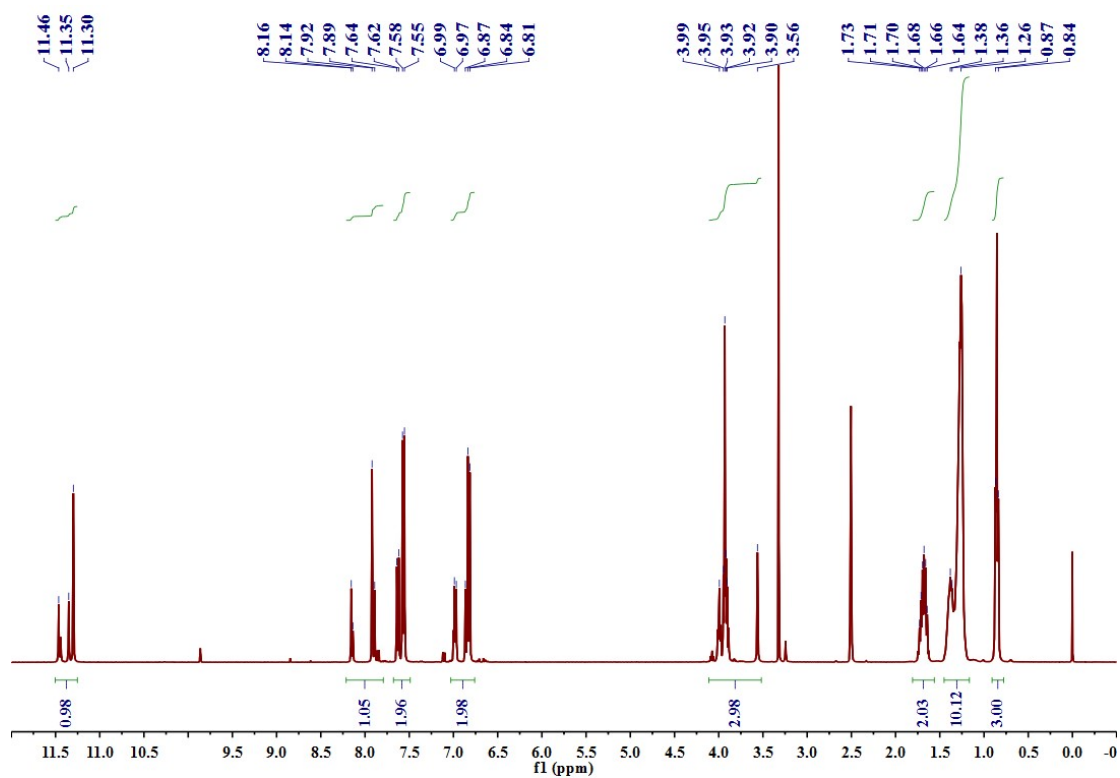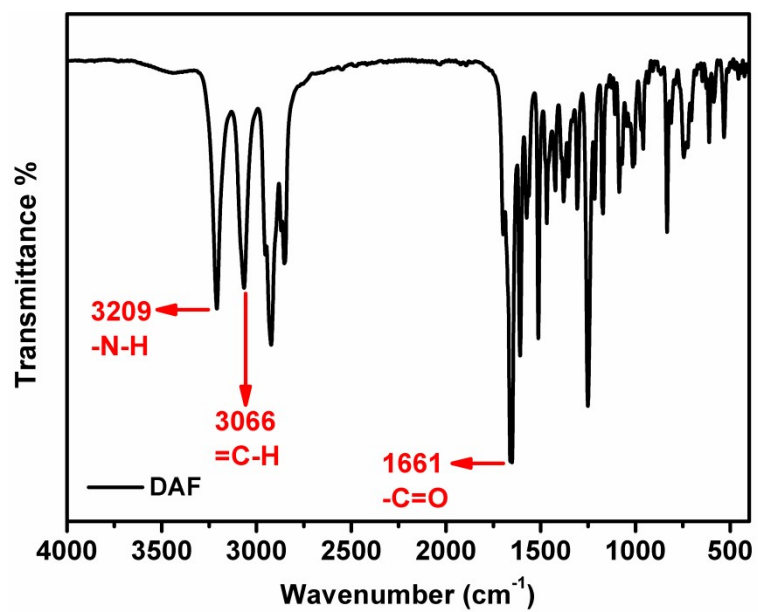
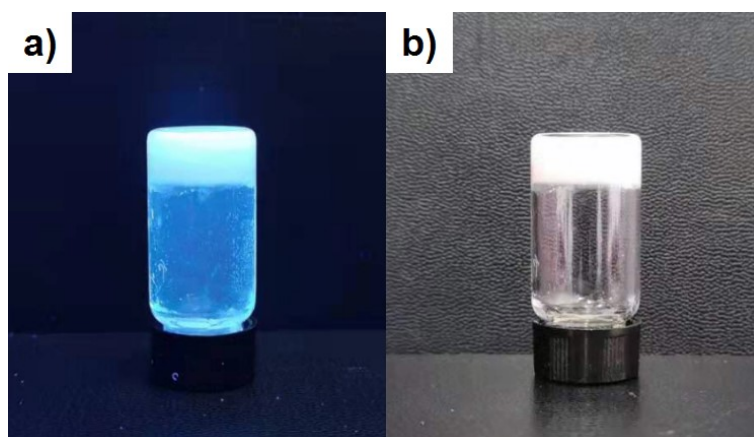**Fig. S1** ^{1}H NMR (400 MHz) spectrum of **DAF** in DMSO-d_6 at 30°C
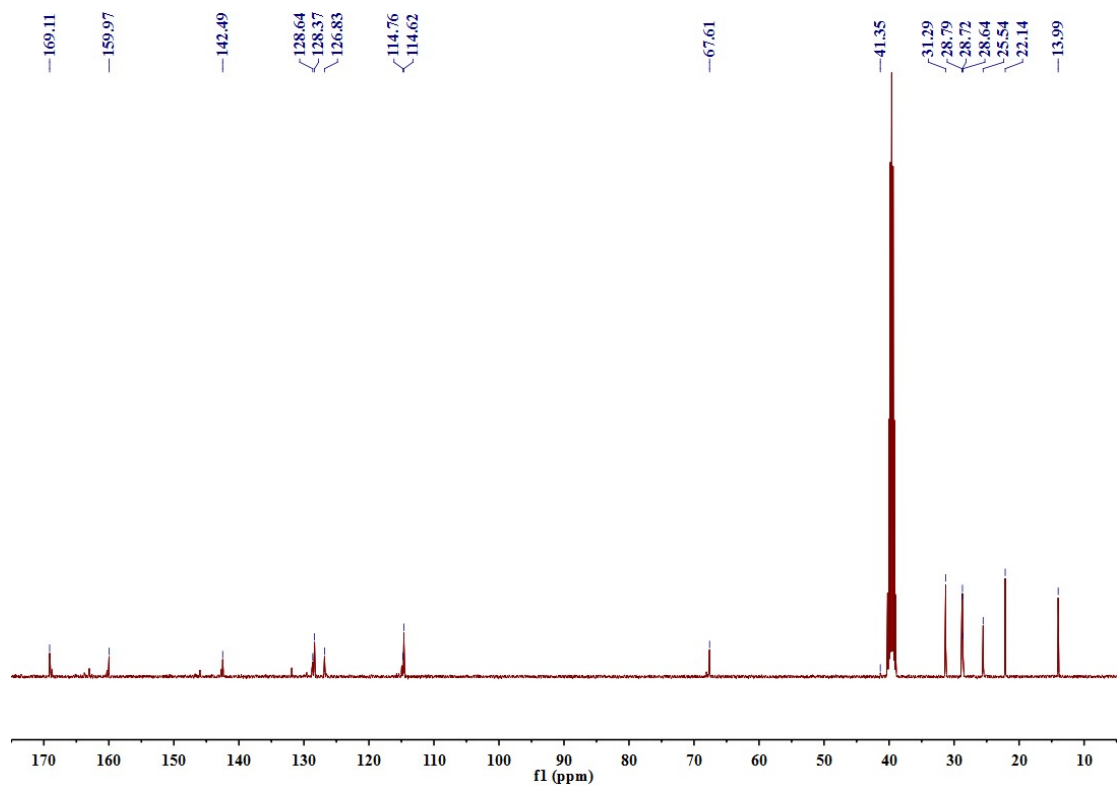
Fig. S2 ^{13}C NMR (100.5 MHz) spectrum of **DAF** in DMSO-d_6 at 30°C
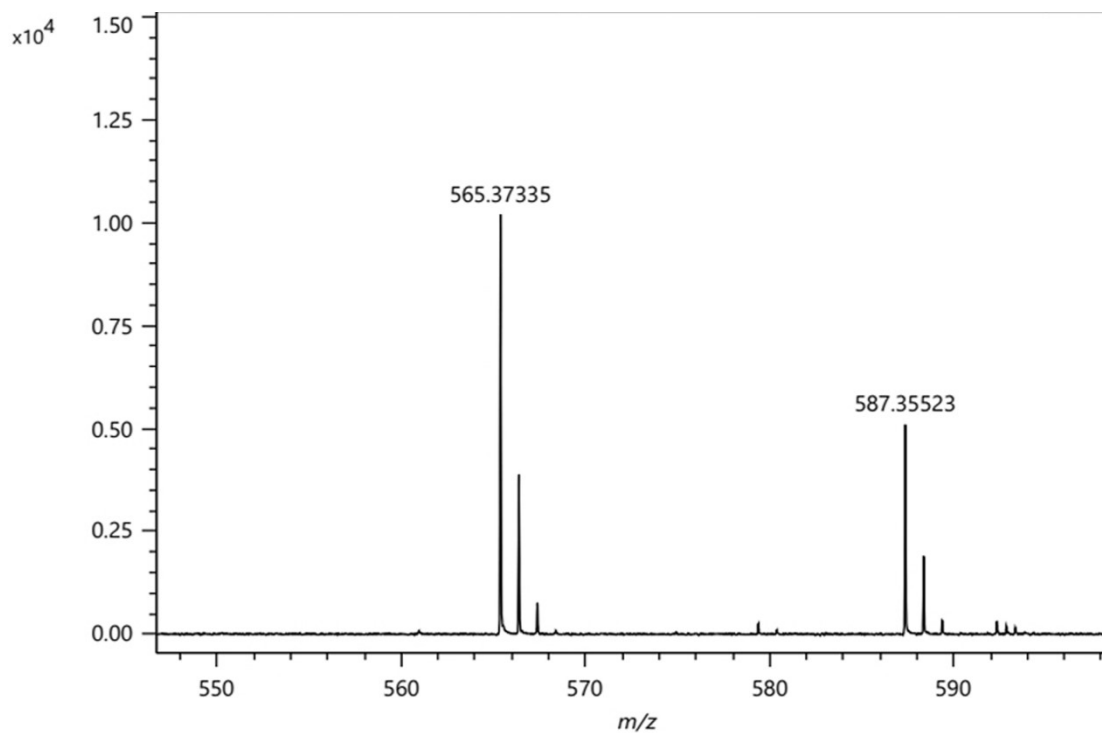
Fig. S3 ESI-MS spectrum of **DAF**

Fig. S4 FT-IR spectra of **DAF**

Fig. S5 Photographs of DAF-gel under illumination at 365 nm and ambient light
(0.8 %, $V_{DMSO} : V_{H2O} = 3 : 7$)

Table S1 Gelation properties of the supramolecular gel **DAFG**

| Entry	Solvent	State[a]	CGC[b](%)	T_{gel}[c] (°C, wt %)
1	Cyclohexane	P	\	\
2	Toluene	S	\	\
3	Toluene-H_2O	P	\	\
4	Petroleum ether	P	\	\
5	Chloroform	S	\	\
6	Chloroform-H_2O	P	\	\
7	Dichloromethane	S	\	\
8	Dichloromethane-H_2O	P	\	\
9	Acetone	P	\	\
10	Acetonitrile	P	\	\
11	DMF	S	\	\
12	DMF-H_2O	G	0.8	85 (0.8%)
13	DMSO	S	\	\
14	DMSO-H_2O	G	0.8	65 (0.8%)
15	Methanol	P	\	\
16	Ethanol	P	\	\
17	Ethanediol	P	\	\
18	Propyl alcohol	P	\	\
19	Isopropanol	P	\	\
20	n-Butyl alcohol	S	\	\
21	n-Butyl alcohol-H_2O	P	\	\
22	n-Amyl alcohol	S	\	\
23	n-Amyl alcohol-H_2O	P	\	\
24	Isoamyl alcohol	S	\	\
25	Isoamyl alcohol-H_2O	P	\	\
26	Hexyl alcohol	S	\	\
27	Hexyl alcohol-H_2O	P	\	\
28	Water	P	\	\
29	CCl_4	P	\	\

[a] G, P and S denote gelation, precipitation and solution, respectively

T$_{sg}$ (gel-sol transition temperature)

For the measurement, a tube inversion method was used for gelation characterization. A capped vial containing the gel was immersed in an oil bath. With the increase of temperature, once gel moving was observed upon the tilting of the vial, an average temperature of three such measurements was defined as the sol-gel transition.
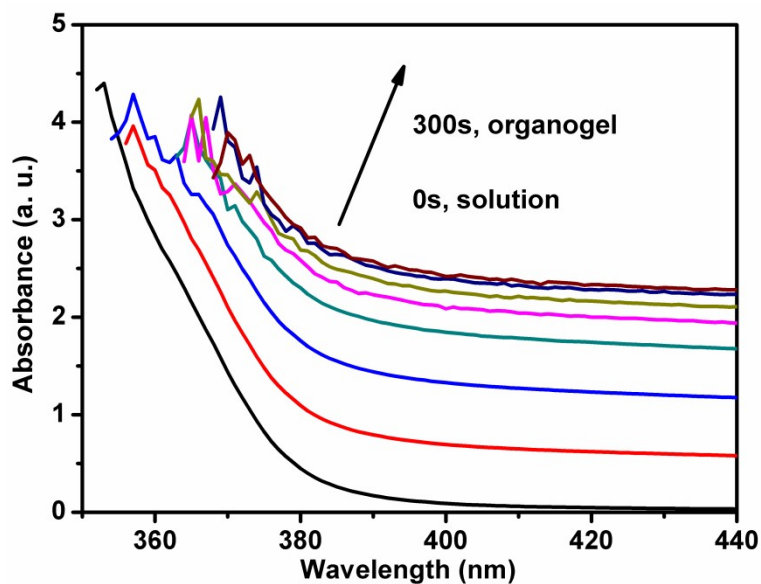
Fig. S6 Time-dependent UV-Vis absorption spectra of organogel **DAFG** (0.3%, V$_{DMSO}$: V$_{H2O}$ = 3 : 7) during the gelation process
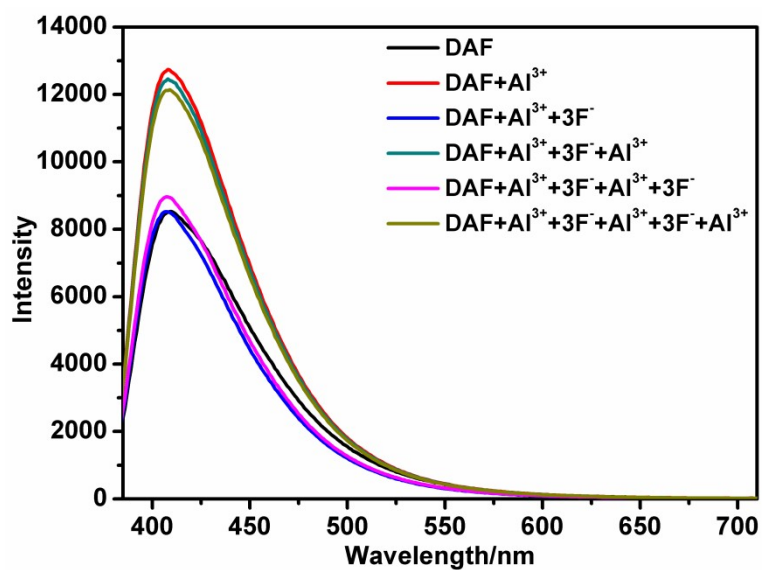
Fig. S7 Fluorescence emission spectra of DAF in the presence of
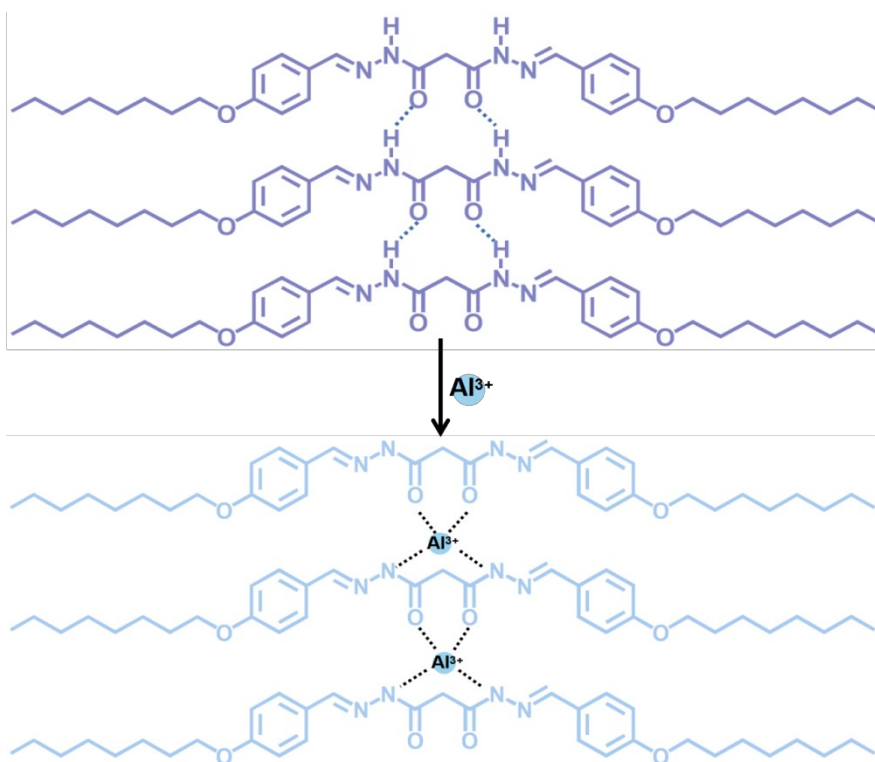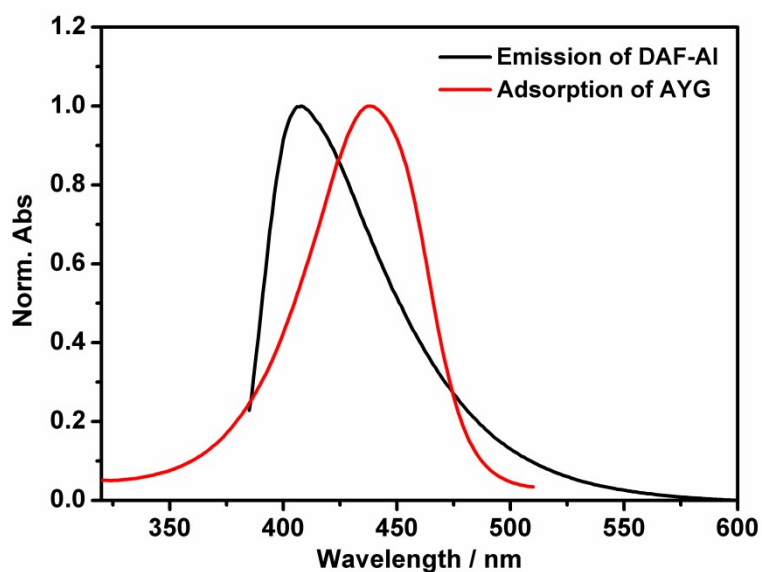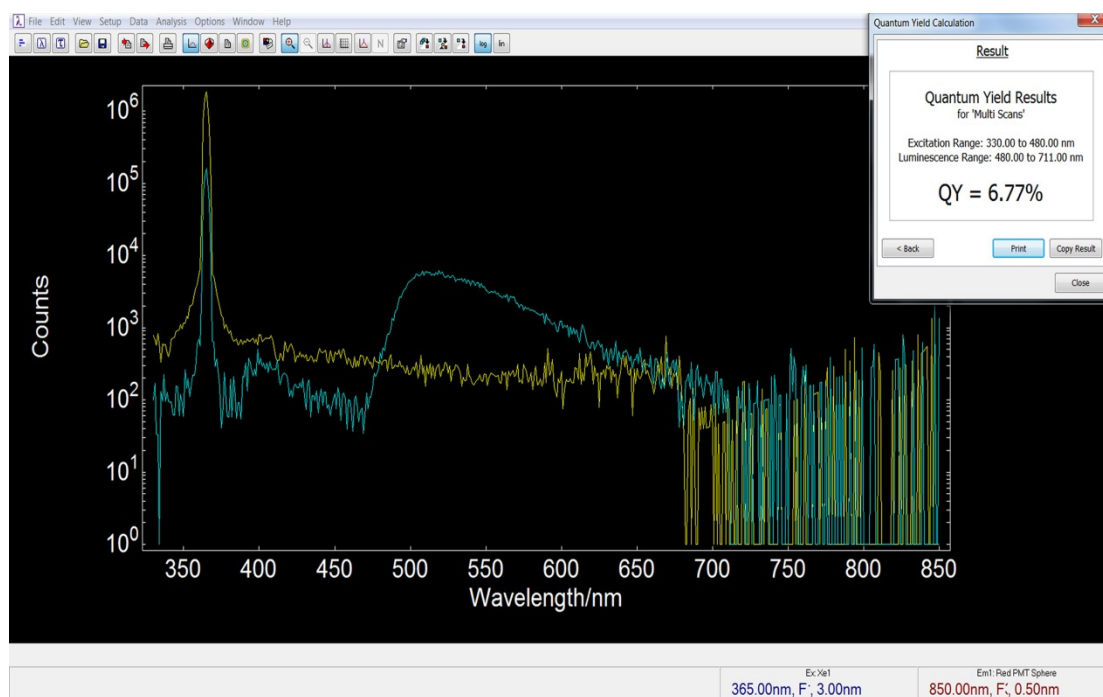Al^{3+} or F^-

Fig. S8 Proposed sensing mechanism of DAF for Al^{3+}

Fig. S9 Normalized emission spectrum of DAF-Al^{3+} (1 × 10^{-2} M), absorption
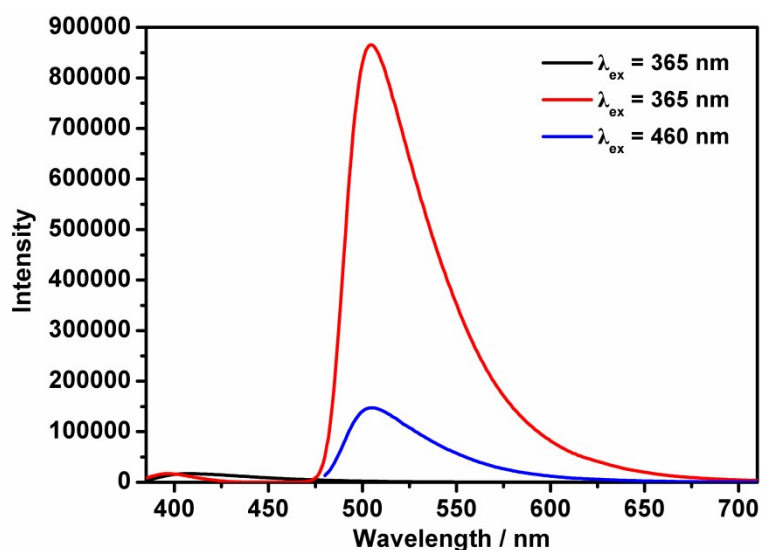
spectrum of AYG (1 × 10^{-5} M)

Fig. S10 Absolute fluorescence quantum yields ($\Phi_{f(abs)}$) of DAF-Al^{3+}-AYG
($n_{DAF-Al}{}^{3+}$: $n_{DAF-Al}{}^{3+}$$_{-AYG}$ = 4 : 1) (λ_{ex} = 365 nm) in DMSO/H$_2$O

Energy-transfer efficiency (Φ_{ET})

Energy-transfer efficiency, Φ_{ET}, the fraction of the absorbed energy that is transferred to the acceptor is experimentally measured as a ratio of the fluorescence intensities of the donor in the absence and presence of the acceptor (I_D and I_{DAF}).[1]

$$\Phi_{ET} = 1 - I_{DA}/I_D$$

Antenna effect (AE) calculation
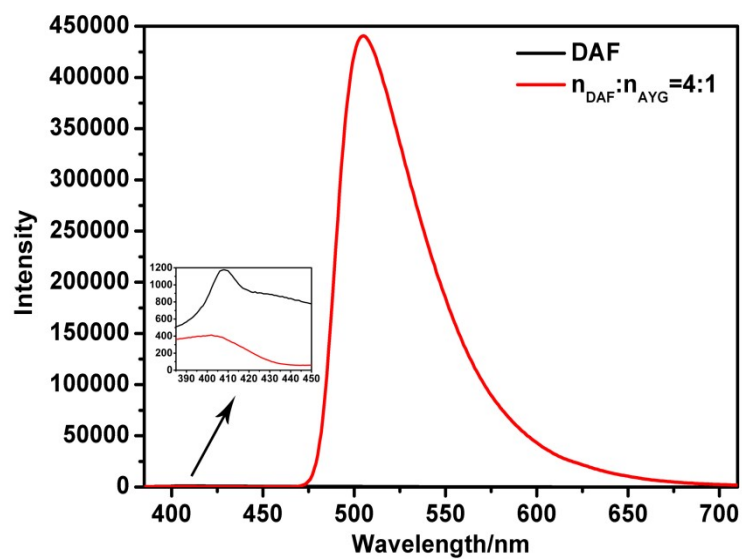

Fig. S11 Fluorescence spectra of DAF-Al^{3+}-AYG (red line), blue line (acceptor emission, λ_{ex} = 460 nm). The black line represents the fluorescence spectrum of DAF-Al^{3+}, which was normalized according to the fluorescence intensity at 410 nm of the red line.

The antenna effect (AE) was calculated based on the excitation spectra using equation S1.[1]

$$AE = (I_{DAF,365} - I_{D,365}) / I_{DAF,460} \text{ (eq. S1)}$$

Where $I_{DAF,365}$ and $I_{DAF,450}$ are the fluorescence intensities at 504 nm with the excitation of the donor at 365 nm and the direct excitation of the acceptor at 460 nm, respectively. $I_{D,365}$ is the fluorescence intensity at 504 nm of the DAF-Al^{3+} assembly, which was normalized with the DAF-Al^{3+}-AYG assembly at 410 nm.

Fig. S12 Fluorescence spectra of DAF (0.8 μM, $V_{DMSO} : V_{H2O} = 9 : 1$) and DAF-AYG ($\lambda_{ex} = 365$ nm, [DAF] = 0.8 μM, [AYG] = 0.2 μM)
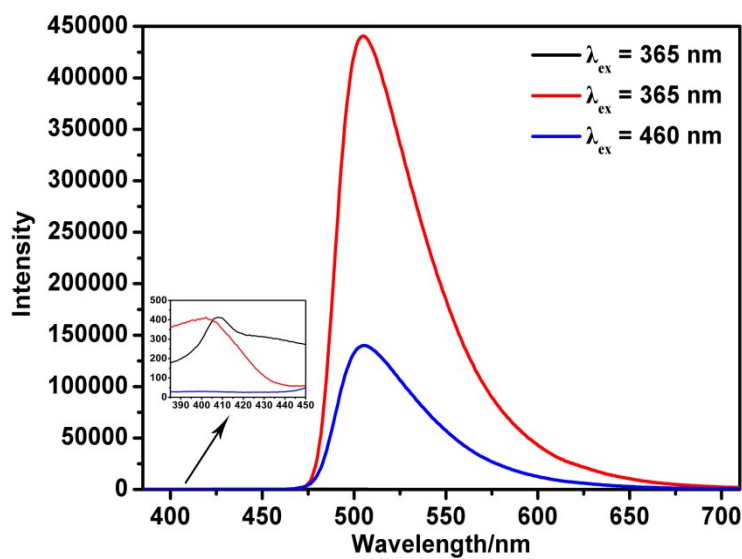
Fig. S13 Fluorescence spectra of DAF-AYG (red line), blue line (acceptor emission, $\lambda_{ex} = 460$ nm). The black line represents the fluorescence spectrum of DAF, which was normalized according to the fluorescence intensity at 404 nm of the red line.
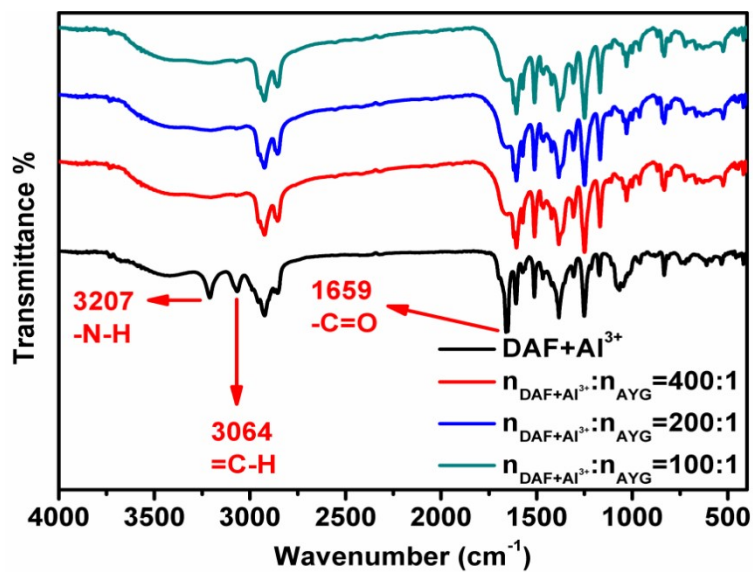
Fig. S14 FT-IR spectra of DAF-Al^{3+} and DAF-Al^{3+}-AYG with different amounts of AYG

References

1. (a) J. J. Li, Y. Chen, J. Yu, N. Cheng and Y. Liu, Adv. Mater., 2017, **29**, 1701905; (b) S. Guo, Y. Song, Y. He, X. Y. Hu and L.Wang, Angew. Chem. Int. Ed., 2018, **57**, 3163; (c) M. Hao, G. P. Sun, M. Z. Zuo, Z. Q. Xu, Y. Chen, X. Y. Hu and L. Y. Wang, Angew. Chem. Int., Ed., 2019, **58**, 2.